Experiments on transition to turbulence in an oscillatory pipe flow

By MIKIO HINO, MASAKI SAWAMOTO
AND SHUJI TAKASU†

Department of Civil Engineering, Tokyo Institute of Technology,
O-okayama, Meguro-ku, Tokyo 152, Japan

Experiments on transition to turbulence in a purely oscillatory pipe flow were performed for values of the Reynolds number R_δ, defined using the Stokes-layer thickness $\delta = (2\nu/\omega)^{\frac{1}{2}}$ and the cross-sectional mean velocity amplitude $\hat{U}$, from 19 to 1530 (or for values of the Reynolds number R_e, defined using the pipe diameter d and $\hat{U}$, from 105 to 5830) and for values of the Stokes parameter $\lambda = \frac{1}{2}d(\omega/2\nu)^{\frac{1}{2}}$ (ν = kinematic viscosity and ω = angular frequency) from 1·35 to 6·19. Three types of turbulent flow regime have been detected: weakly turbulent flow, conditionally turbulent flow and fully turbulent flow. Demarcation of the flow regimes is possible on R_δ, λ or R_e, λ diagrams. The critical Reynolds number of the first transition decreases as the Stokes parameter increases. In the conditionally turbulent flow, turbulence is generated suddenly in the decelerating phase and the profile of the velocity distribution changes drastically. In the accelerating phase, the flow recovers to laminar. This type of partially turbulent flow persists even at Reynolds numbers as high as $R_e = 5830$ if the value of the Stokes parameter is high.

1. Introduction

A variety of problems concerning turbulent oscillatory flow are frequently encountered in the applied fields of fluid mechanics. Among these problems are the boundary layer on a channel bottom produced by progressive water waves and the oscillation of water columns in pipes caused by surging or a water hammer.

Transition to turbulence is one of the important aspects of purely oscillatory flow. Nevertheless, few papers, either theoretical or experimental, have been published on purely oscillatory flow instability, in comparison with the large number of investigations of oscillatory perturbing flow superposed on a steady main flow (see, for example, Eichelbrenner 1972). Experiments on oscillatory flow instability have been carried out by Li (1954) for the Stokes layer on smooth and rough plates, by Collins (1963) for the modified Stokes layer induced by progressive surface waves and by Sergeev (1966) for oscillatory pipe flow. The

† Present address: Public Works Research Institute, Ministry of Construction, Shinozaki, Edogawa, Tokyo 133, Japan.

critical Reynolds number based on the Stokes-layer thickness ($R_\delta^* = U_0 \delta/\nu$, $\delta = (2\nu/\omega)^{\frac{1}{2}}$, where U_0 and ω are the velocity amplitude on the axis and angular frequency of the harmonic motion, respectively) has been determined to be $R_\delta^* = 565$ for the Stokes layer on a smooth wall, a significantly lower value of $R_\delta^* = 160$ for the modified Stokes layer or wave boundary layer, and $R_\delta = 500$ ($R_\delta = \hat{U}\delta/\nu$, $\hat{U}$ = mean velocity amplitude) for oscillatory pipe flow. Experiments by Hino & Takasu (1974) showed that purely oscillatory pipe flows are more stable than unidirectional steady flow and can be turbulent during only part of each cycle, decaying suddenly when the direction of flow is reversed. Recently, after in oscillating flows submission of the first draft of our paper, experimental results on transition in a *closed pipe* at higher frequencies ranging from 10 to 130 Hz have been presented by Merkli & Thomann (1975), who also confirmed the occurrence of periodic bursts.

The instability of purely oscillatory flows has been analysed theoretically by Conrad & Criminale (1965), von Kerczek & Davis (1972) and Davis & von Kerczek (1973) by means of energy stability theory, by Collins (1963) on the basis of the quasi-static assumption, and by von Kerczek & Davis (1974) using quasi-static linear theories and an integration of the full time-dependent linearized disturbance equations. The energy theories give a relatively low critical Reynolds number sufficient for stability (R_δ^* about $40 \sim 50$ for two-dimensional disturbances), while the full theory of von Kerczek & Davis predicts absolute stability within the investigated range ($R_\delta^* < 800$) and perhaps for all Reynolds numbers. Hino & Sawamoto (1975a) have carried out a preliminary time-dependent linear stability analysis by the double Galerkin method and obtained the result $R_\delta = 260$ for the critical Reynolds number for $\lambda = 3.54$.

2. Experimental apparatus

The present work was conducted in lucite circular pipes having inner diameters of 14.5 and 29.7 mm and lengths of 400 cm for most experimental runs and 600 cm for a few runs. The pipes were connected through bell-shaped smooth transitions to an outlet at one end and to a piston chamber (I.D. 30 or 78 mm) at the other end. The general arrangement of the equipment is shown in figure 1.

The piston was driven by a constant-speed electric motor whose rotating period was varied by exchanging the gear-box attachment. Rotary motion of the arm fixed on the axis of the motor-gear system was converted to a transversely sliding one by mechanically projecting it onto the arm of the piston. Several combinations of gear box, length of rotating arm, diameter of the pipes and diameter of the piston chamber allowed the Reynolds number defined in terms of the oscillating mean velocity amplitude $\hat{U}$ and pipe diameter d ($R_e = \hat{U}d/\nu$) to vary from 105 to 5830, the Reynolds number defined in terms of $\hat{U}$ and the Stokes-layer thickness $\delta = (2\nu/\omega)^{\frac{1}{2}}$ ($R_\delta = \hat{U}\delta/\nu$, which is related to R_e by $R_e = 2\lambda R_\delta$) to vary from 19 to 1530 and the Stokes parameter λ (which is the ratio of the radius to the Stokes boundary-layer thickness and is defined by $\lambda = \frac{1}{2}d(\omega/2\nu)^{\frac{1}{2}}$, $\omega = 2\pi/T$, T = period of oscillating motion) to vary from 1.91 to 6.19, as summarized in table 1.
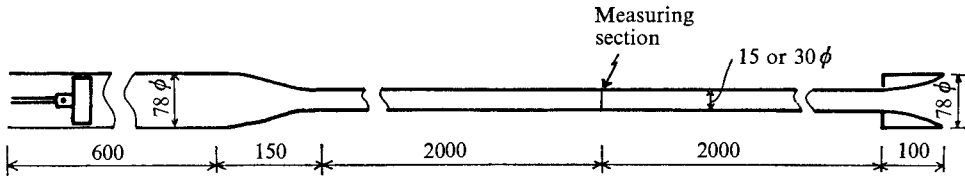
FIGURE 1. A schematic diagram of the apparatus. Dimensions in mm.

Run	Pipe diameter d (mm)	Period T (s)	Amplitude of cross-sectional mean velocity variation $\hat{U}$ (m/s)	$R_e = \dfrac{\hat{U}d}{\nu}$	$\lambda = \left(\dfrac{\omega}{2\nu}\right)^{\frac{1}{2}}\dfrac{d}{2}$	$R_\delta = \dfrac{\hat{U}\delta}{\nu}$	Flow regime	Figure
1	30	6·0	0·053	105	2·76	19	○	—
2	30	6·0	0·105	210	2·76	38	○	—
3	30	6·0	0·158	315	2·76	57	○	—
4	30	6·0	0·355	710	2·76	128	○	3(a)
5	30	6·0	0·710	1420	2·76	256	○	—
6	30	6·0	1·065	2130	2·76	386	●	4(a)
7	30	3·0	0·710	1420	3·90	180	●	4(b)
8	30	3·0	1·42	2840	3·90	361	●	—
9	30	3·0	2·13	4260	3·90	568	●	6(a)
11	14·5	3·0	1·81	1750	1·91	460	○	3(b)
12	14·5	3·0	2·20	2070	1·91	543	✦	6(b)
13	14·5	3·0	4·38	4230	1·91	1110	✦	—
14	14·5	3·0	6·03	5830	1·91	1530	✦	6(c)
15	14·5	6·0	1·83	1770	1·35	660	○	—
16	14·5	6·0	2·97	2870	1·35	1060	● or ✦	—
17	30	1·2	0·425	850	6·19	69	●	—
18	30	2·4	0·225	450	4·45	51	○	—
19	30	2·4	0·30	600	4·45	67	○	—
20	30	2·4	0·40	800	4·45	90	●	—
21	30	4·8	0·435	870	3·12	140	○	—
22	30	4·8	0·660	1320	3·12	212	○	—
23	30	4·8	0·875	1750	3·12	281	●	—
24	30	4·8	1·31	2620	3·12	420	●	—
25	30	6·0	0·875	1750	2·76	368	●	—

TABLE 1. Summary of the experimental conditions

Velocity was measured by a constant-temperature hot-wire anemometer (Nihon Kagaku Kogyo Co.). The probe was inserted into the tube through a small hole of diameter 6 mm opened in the middle of the pipe.

It should be pointed out that at a velocity close to zero the response of the anemometer would change since the heat transfer from a hot wire is due to free convection and not to forced convection. Output from the hot-wire electronic channel was recorded photographically on oscillograph paper. The anemometer signals were calibrated *in situ* by rotating-arm equipment in a closed chamber.

Linearity was held to a velocity as low as 6 cm/s. It was anticipated also that the wake produced by the probe itself would contaminate the record of velocity when the direction of flow reversed. However, a preliminary experiment on the effect using a dummy probe showed that the turbulence produced by the probe disappeared immediately in the reversed-flow stage (Hino & Sawamoto 1975b). Moreover, for velocity measurements with a hot wire in flows of zero mean value, interference of the thermal wake with the measurements may be present. On this point, Merkli & Thomann (1975) state that the disturbances of the flow by the hot-wire probe become larger for higher frequencies as high as 85 Hz and vanish for lower ones. Our experiment has been performed at lower frequencies of at most $\frac{1}{8}$–1 Hz. Repetition of experiments on transitional and turbulent oscillatory flows with a non-touch type of advanced anemometer, for instance a laser-beam or sonic anemometer, might be of value.

3. Experimental results on transition to turbulence in purely oscillatory flow

Laminar flow at low Reynolds numbers

When R_e is as low as a few hundred, the results of experiments coincide well with the theoretical prediction for laminar flow. The velocity distribution under the pressure gradient $-\rho^{-1}\partial p/\partial z = K e^{i\omega t}$ is given (see, for example, Rosenhead 1963, p. 388) by

$$u(r,t) = R\{U(\eta,\lambda) e^{i\tau}\} = R\{|U(\eta,\lambda)| e^{i(\tau+\theta)}\}, \tag{1}$$

where

$$U(\eta,\lambda) = -iK\omega^{-1}[1 - J_0(\alpha\lambda\eta)/J_0(\alpha\lambda)], \tag{2}$$

and

$$\tau = \omega t, \quad \eta = 2r/d, \quad \alpha = 2^{\frac{1}{2}} e^{\frac{3}{4}\pi i}.$$

The amplitude of the mean velocity across the cross-section is given by

$$\hat{U} = K\omega^{-1}|1 - (2/\alpha\lambda) J_1(\alpha\lambda)/J_0(\alpha\lambda)|. \tag{3}$$

In these expressions, d is the pipe diameter, r the radial co-ordinate, and θ the phase lag. Figure 2 shows plots of $U/\hat{U}$ and θ as functions of η, for $\lambda = 2\cdot76$, and experimental results for $R_\delta = 19$, 38 and 57 ($R_e = 105$, 210 and 315). Since at these low Reynolds numbers the maximum velocity was as low as 27 cm/s even for $R_e = 315$, the output signals suffered a little from noise. The oscillograph records were Fourier analysed after calibration to show that the flows were completely sinusoidal, assuring the reliability of the driving mechanism.

When the Reynolds number is increased to $R_\delta = 128$ ($R_e = 710$) keeping the Stokes parameter at the same value ($\lambda = 2\cdot76$), the profiles of velocity distribution begin to deviate slightly from the theoretical one for laminar flow at the central position of the pipe. Figure 3(a) is constructed to show the profile distortion by plotting on the same abscissa (the ordinate being displaced vertically by equal distances) the oscillograph traces obtained at several radial positions equally spaced from the pipe axis (the uppermost curve) to the wall (the lowest curve). These curves were obtained not simultaneously but independently. Moreover, the ordinate is the absolute velocity since the anemometer cannot
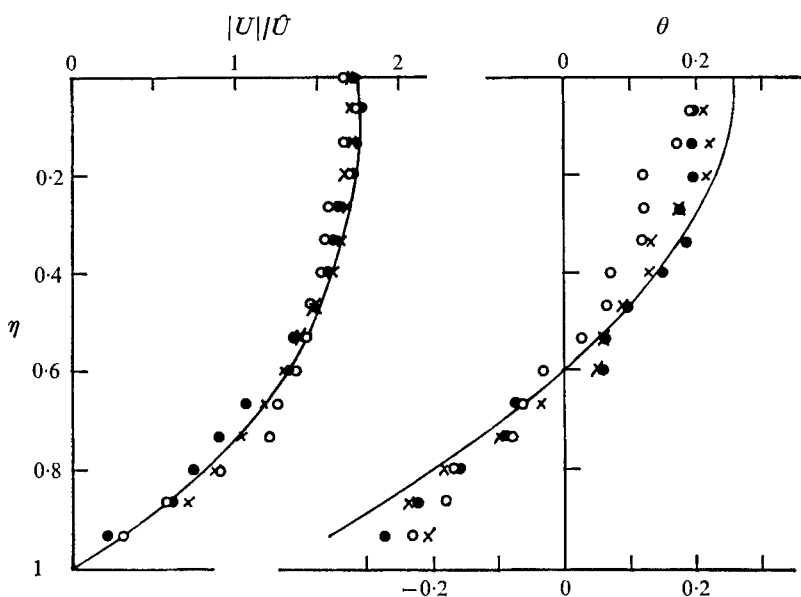
FIGURE 2. Comparison between theory and experiments (runs 1–3) on the velocity distribution for laminar oscillatory pipe flows. $\bigcirc$, $R_e = 105$, $R_\delta = 19$; $\bullet$, $R_e = 210$, $R_\delta = 38$; $\times$, $R_e = 315$, $R_\delta = 57$. $\lambda = 2\cdot76$.

detect the flow direction. Though these curves are not linearized, they may be considered to give the real velocities because the distortion of the signal from conditions of linearity is very low. As is evident from figure 3(a), the velocity profiles are distorted a little during the initial stage of flow reversal at the central position of the pipe. However, on the whole, the amplitude of the velocity and the phase lag coincide with the theory of laminar flow.

At the same value of λ a further increase in the Reynolds number gives rise to the initiation of turbulence, to be discussed in the next subsection. However, at lower values of λ, the flow remains laminar or distorted laminar for much higher values of R_δ (runs 11 and 15 in table 1). Figure 3(b) shows a result for $\lambda = 1\cdot91$ ($R_\delta = 460$).

Weakly turbulent flow at transition Reynolds numbers

As stated previously, the velocity distributions distort in part from laminar at a relatively low Reynolds number R_δ of 128 ($R_e = 710$) when $\lambda = 2\cdot76$. If the Reynolds number is increased, keeping λ ($= 2\cdot76$) unchanged, to $R_\delta = 380$ ($R_e = 2130$), small amplitude perturbations are superposed on the distorted laminar flow as shown in figure 4(a).

If λ is increased to $3\cdot90$, the same type of transition is observed at a lower Reynolds number $R_\delta = 180$ ($R_e = 1420$, figure 4b) and continues at Reynolds numbers as high as $R_\delta = 361$ ($R_e = 2840$). Dominance of this type of flow for a wide range of R_e may be confirmed from figure 5, in which experimental results for $|U|/\hat{U}$ and θ for two runs at low and high Reynolds numbers coincide well with each other. In figure 5, on the one hand the distributions of amplitude of
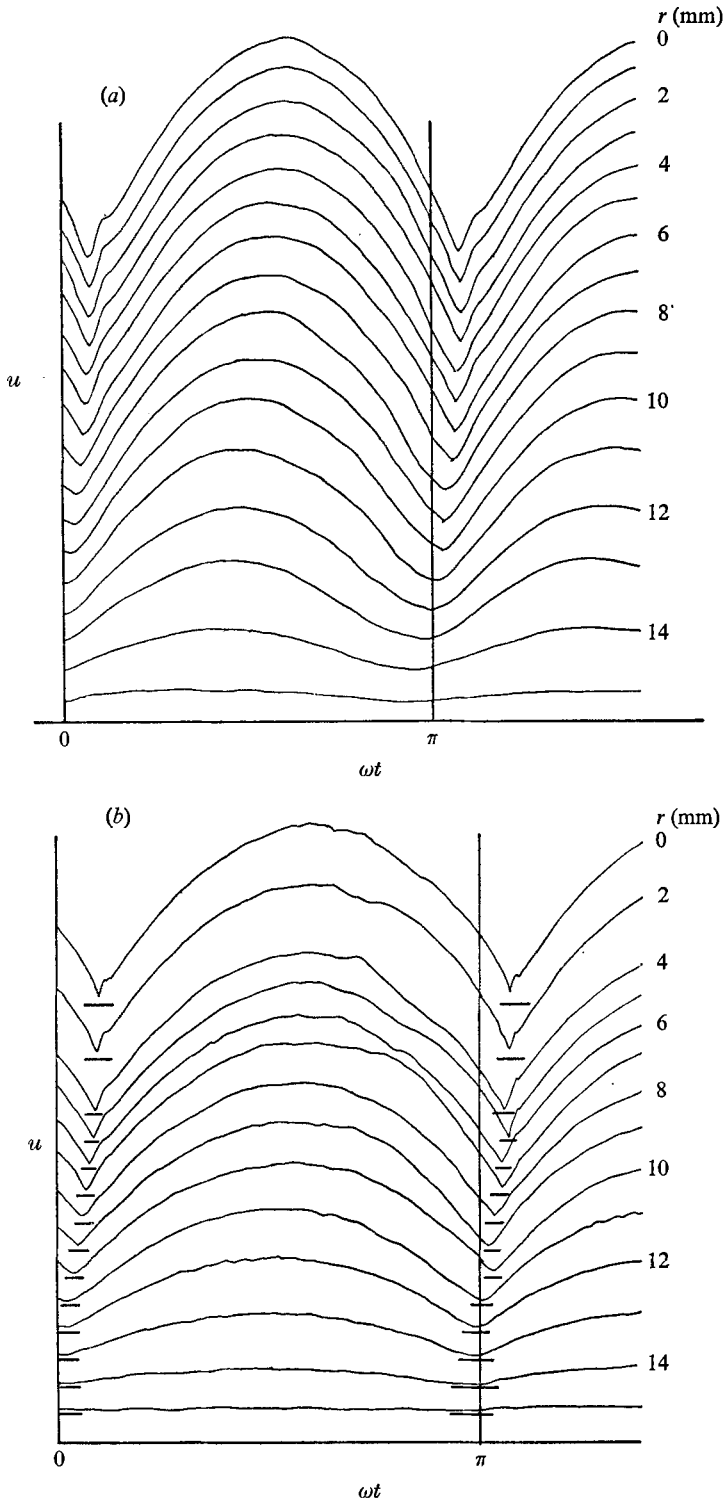
FIGURE 3. Traces of the velocity variation at various radial positions. (a) $R_\delta = 128$ ($R_e = 710$) and $\lambda = 2\cdot76$ ($\hat{U} = 0\cdot35$ m/s, $T = 6\cdot0$ s, $d = 3\cdot0$ cm); run 4. (b) $R_\delta = 460$ ($R_e = 1750$) and $\lambda = 1\cdot91$ ($\hat{U} = 1\cdot81$ m/s and $T = 3\cdot0$ s, $d = 1\cdot45$ cm); run 11.
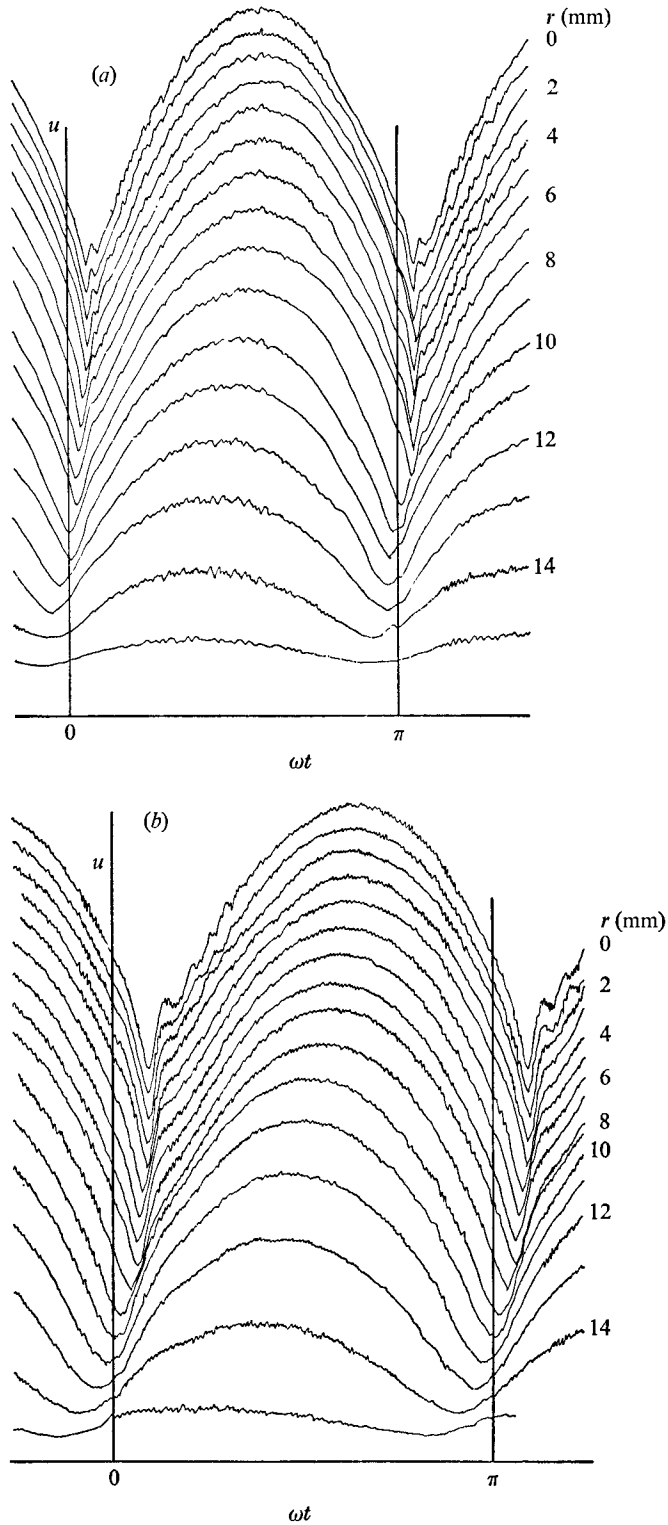
FIGURE 4. Traces of velocity variation in a weakly turbulent oscillatory pipe flow. (*a*)
$R_\delta = 386$ ($R_e = 2130$) and $\lambda = 2.76$ ($\hat{U} = 1.07$ m/s, $T = 6.0$ s, $d = 3.0$ cm); run 6.
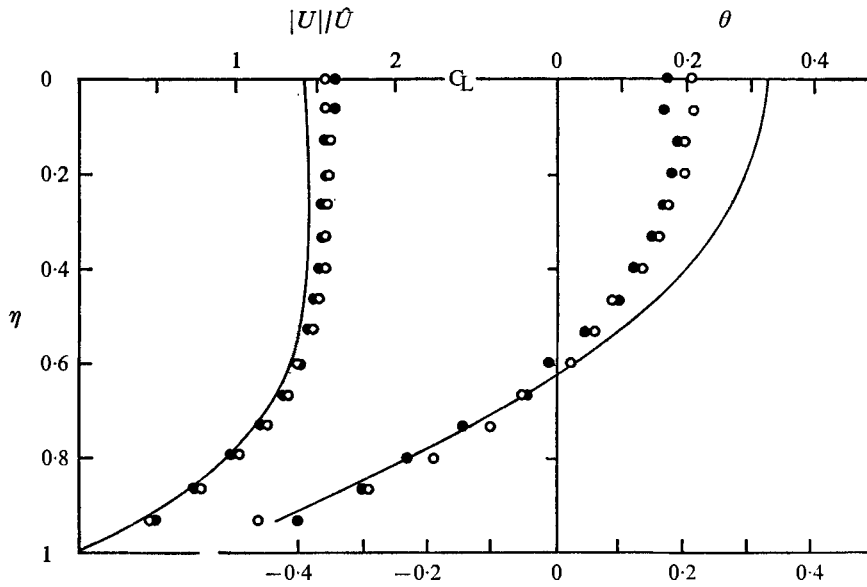(*b*) $R_\delta = 180$ ($R_e = 1420$) and $\lambda = 3.90$ ($\hat{U} = 0.7$ m/s, $T = 3.0$ s, $d = 3.0$ cm); run 7.

FIGURE 5. Velocity distributions in weakly turbulent oscillatory pipe flows compared, for reference, with the theoretical curve for laminar flow. $\bigcirc$, $R_\delta = 180$ ($R_e = 1420$), $\lambda = 3.90$; $\bullet$, $R_\delta = 361$ ($R_e = 2840$), $\lambda = 3.90$).
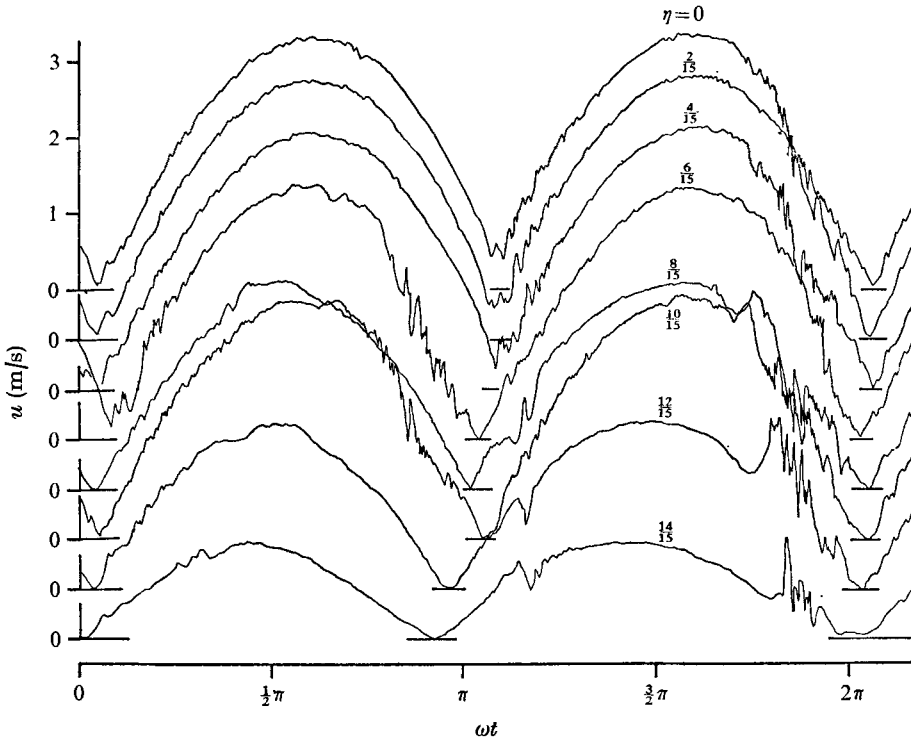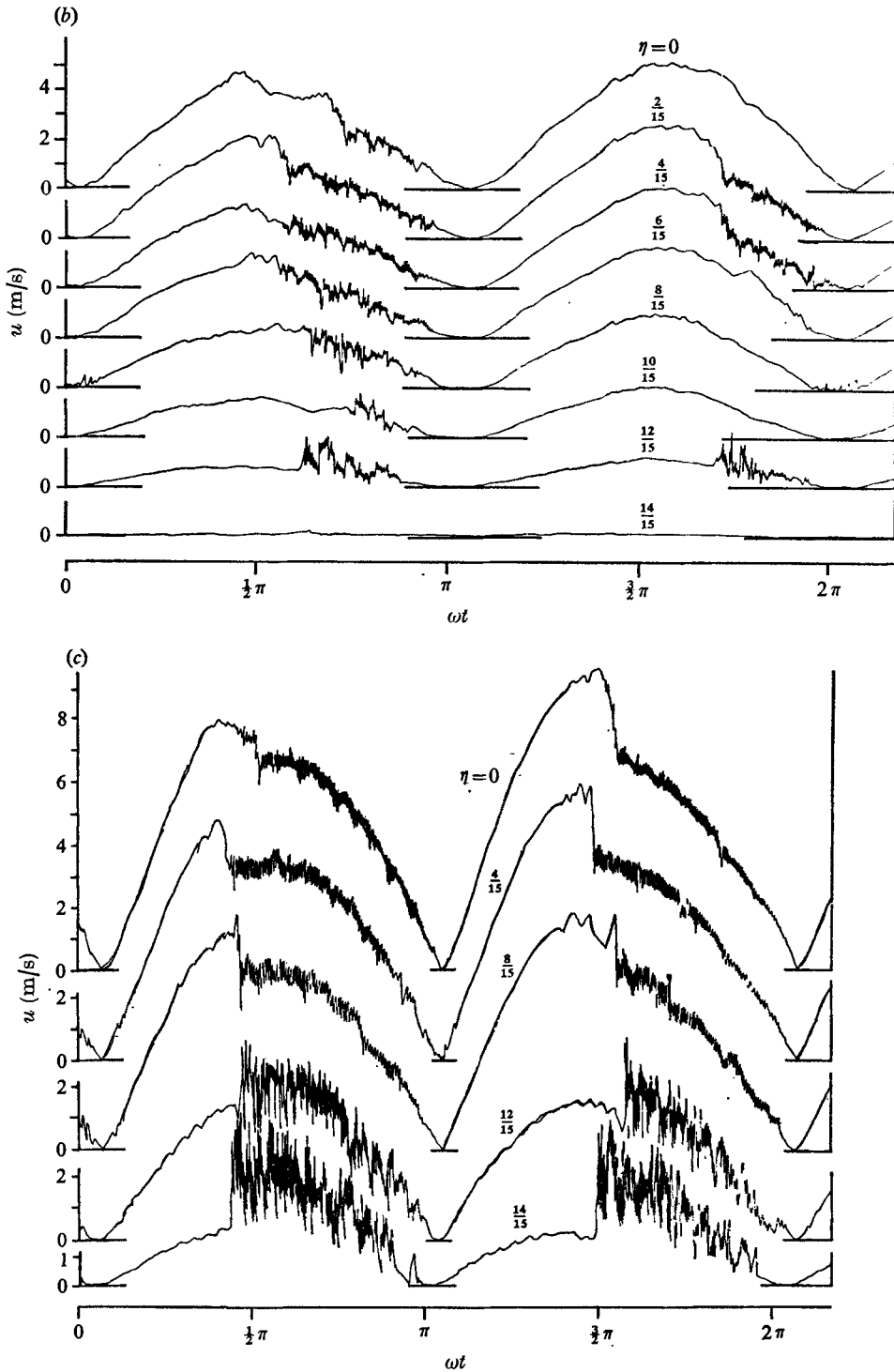

FIGURE 6(a). For legend see facing page.

FIGURE 6. Traces of velocity variation. (a) $R_\delta = 568$ ($R_e = 4260$) and $\lambda = 3.90$ ($\hat{U} = 2.13$ m/s, $T = 3.0$ s, $d = 3.0$ cm); run 9. (b) Conditionally turbulent oscillatory pipe flows: $R_\delta = 543$ ($R_e = 2070$) and $\lambda = 1.91$ ($\hat{U} = 2.20$ m/s, $T = 3.0$ s, $d = 1.45$ cm); run 12. (c) $R_\delta = 1530$ ($R_e = 5830$) and $\lambda = 1.91$ ($\hat{U} = 6.03$ m/s, $T = 3.0$ s, $d = 1.45$ cm); run 14.

velocity variation agree well with the theoretical curve of laminar oscillatory flow, on the other hand the phase lag distributions differ considerably from it in the central portion of the pipe.

Conditional turbulence at higher Reynolds numbers

When the value of R_δ is increased further to $R_\delta = 568$ ($\lambda = 3.90$), a different type of turbulence is realized as shown in figure 6(a). A change in the velocity perturbation pattern at about $R_\delta \simeq 550$ becomes evident as λ decreases (figure 6b). The velocity distributions are disturbed at peaks by a fluctuation of low frequency and high amplitude compared with that in the regime stated above. The second critical Reynolds number of $R_\delta \simeq 550$ seems to be a universal value almost independent of λ. For the case $\lambda = 1.91$, while the flow is distorted laminar at $R_\delta = 460$, it becomes turbulent and of this type at $R_\delta = 543$; for $\lambda = 3.90$ the flow is weakly turbulent at $R_\delta = 361$ and partially turbulent at $R_\delta = 568$. However, the flow for $R_\delta = 660$ is still laminar at the small value of $\lambda = 1.35$ (run 15). Therefore, the critical Reynolds number $R_\delta \simeq 550$ applies only for λ larger than 1.6, as indicated by figure 8(b). Such disturbances are intensified at higher values of R_δ (figure 6c). The flow regime may be described as *conditional turbulence* since turbulence appears only in the decelerating phase, while in the accelerating phase the flow recovers to laminar-like flow.

Figure 7, in which circles denote measurements of the ensemble-average velocity $\langle u(r,t) \rangle$, is shown to compare these with the theoretical laminar oscillatory flow. In the decelerating stage, the velocity at the central position decreases suddenly, accompanied by violent turbulent fluctuations, while near the wall, the velocity increases rapidly above the laminar value, confirming the generation of large-scale eddies across the pipe section.

Stability diagram

The types of oscillatory flow may be classified in terms of the Reynolds number R_e or R_δ and Stokes parameter λ into (a) laminar flow, (b) distorted laminar flow, (c) weakly turbulent flow, (d) conditional turbulence and probably (e) fully turbulent flow, which has not been confirmed in our present data because of limitations of the experimental apparatus. The experimental results are summarized in the stability diagram on λ, R_e or λ, R_δ plots (figures 8a, b). In these figures, open circles mean the laminar regime (a) and (b), solid circles represent weakly turbulent flow (c) and solid circles with a cross stand for conditional turbulence (d).

The first transition from laminar flow to (b) or (c) appears in the accelerating period. In figure 9, a contour map of the velocity distribution is represented on graph of ωt against η. The region enclosed by the dot–dash line, where $u = 0$ in real data, and by the broken line, where from oscillograph records $\partial u/\partial r = 0$, is the region in which $\partial u/\partial r < 0$. Solid lines, which are contour lines for the theoretical laminar flow, are drawn for reference, showing deviation from real ones. Distorted laminar flow, marked by open circles, and weak turbulence, denoted by solid circles, are noticeable in the region where the instantaneous velocity increases radically from the axis ($\partial |u|/\partial r > 0$). The critical Reynolds number for
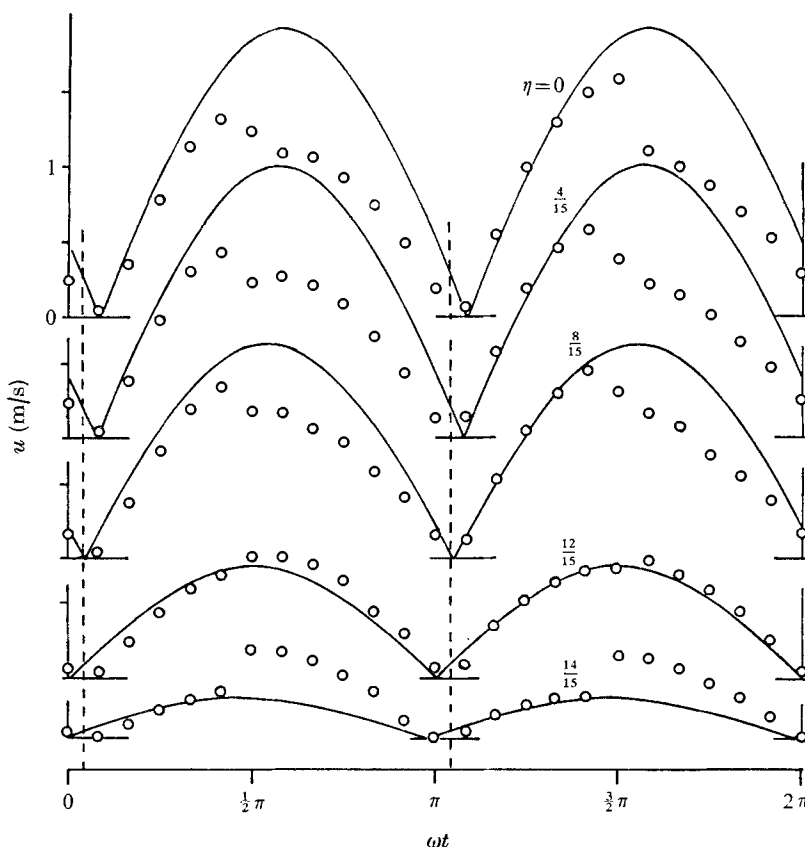
FIGURE 7. Experimental velocity variations compared with the theoretical curves for laminar flow. $R_\delta = 1530$ ($R_e = 5830$) and $\lambda = 1\cdot91$ ($\hat{U} = 6\cdot03$ m/s, $T = 3\cdot0$ s, $d = 1\cdot45$ cm); run 14.

this type of instability of laminar oscillatory flow decreases as the Stokes parameter λ increases.

As the Reynolds number is increased further, the flow becomes conditionally turbulent, in which on the one hand violent turbulence with higher frequency is generated in the decelerating period, and on the other hand the turbulence disappears suddenly in the reversed accelerating period. Although the number of points is scarce because of limitations of our experimental apparatus, the demarcation curves are tentatively drawn on the R_e, λ and R_δ, λ diagrams (figure 8a, b).

The second type of transition in the regime (d) seems to have a close connexion with the phenomenon of relaminarization or reverse transition, which is of current interest. In the accelerating phase, turbulent energy generated in the decelerating phase is transferred back to the main flow.

In our experiment, the effect of viscosity is confined to a thin Stokes layer on the wall, i.e. λ is substantially greater than unity. Thus the Reynolds number R_δ is adequate for the criterion for transition from laminar to turbulent flow.
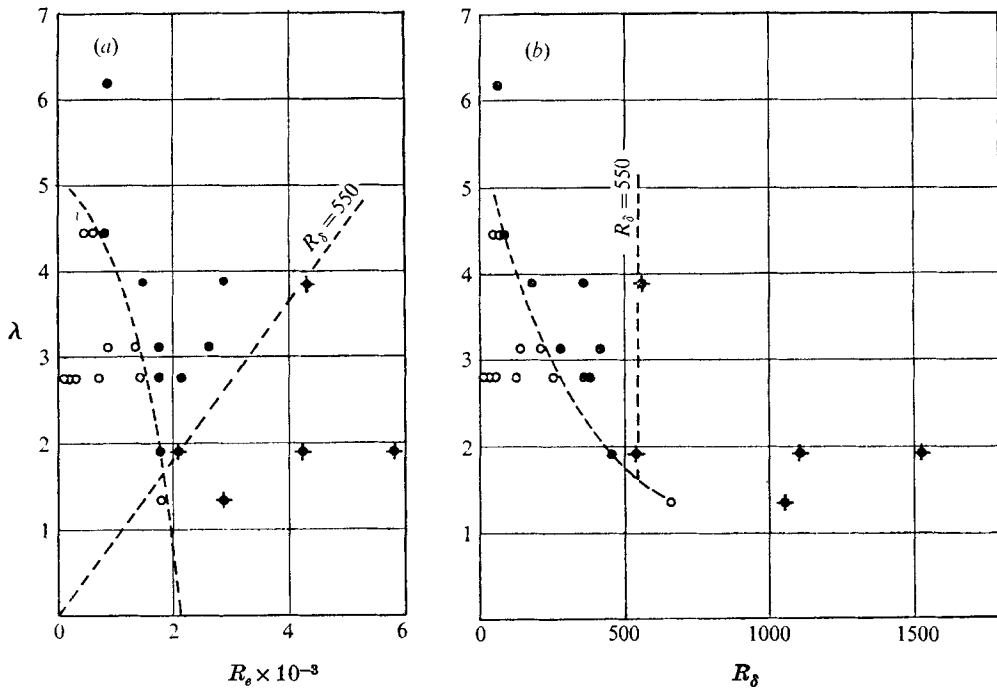
FIGURE 8. Stability diagrams: (a) R_e vs. λ and (b) R_δ vs. λ. ○, laminar or distorted laminar flows; ●, turbulent flow of type (c), i.e. weakly turbulent; ✦, turbulent flow of type (d), i.e. conditionally turbulent.
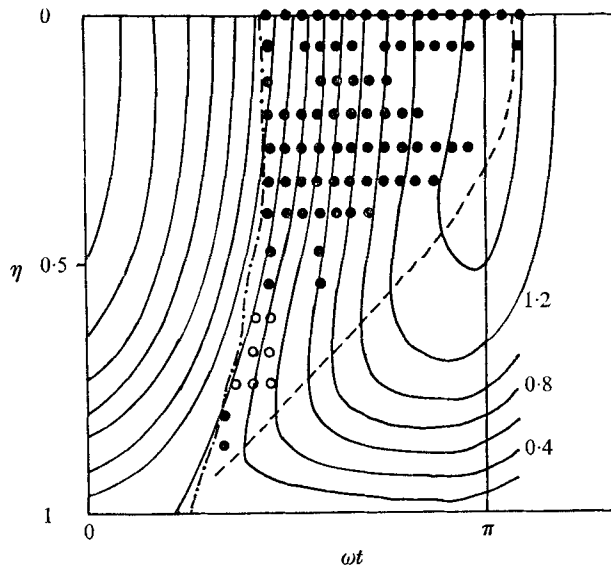

FIGURE 9. Contour map of velocity distribution: ωt vs. η. The types of disturbances: ○, distorted laminar; ●, weak turbulence. ——, theoretical laminar; – – –, $\partial u/\partial r = 0$; —·—, $u = 0$ (measured). $R_\delta = 361$ ($R_e = 2840$) and $\lambda = 3\cdot90$ ($\hat{U} = 1\cdot42$ m/s, $T = 3\cdot0$ s, $d = 3\cdot0$ cm); run 8.

Authors	Condition of experiments and theories	Critical Reynolds number $R_\delta = \hat{U}\delta/\nu$	$R_\delta^* = U_0\delta/\nu$	Stokes parameter, λ	Remarks
Experiments					
Sergeev (1966)	Circular pipe	500	—	2·8–28	Visualization, power measurement
Present authors	Circular pipe	550	—	1·35–6·19	Hot wire
Merkli & Thomann (1975)	Resonant tube	—	290	30–50	Hot wire, visualization
Vincent (1957)	Wave boundary layer	—	110	∞	Dye dispersion
Collins (1963)	Wave boundary layer on smooth plate	—	160	∞	Mass transport velocity
Li (1954)	Oscillating plate in still water	—	565	∞	Dye dispersion
Riedel et al. (1972)	Oscillatory boundary layer	—	135 ~ 1100	∞	Skin-friction measurement
Theory					
Davis & von Kerczek (1973)	Finite Stokes layer	—	2D 3D 264 125 121 58·4 77·6 38·1 61·4 30·5 46·6 24·2	1 2 3 4 ∞	Energy stability theory
Hino & Sawamoto (1975a)	Oscillatory two-dimensional Poiseuille flow between parallel plates	260	315	3.54	Linear stability theory (double Galerkin method)

TABLE 2. Summary of experimental and theoretical results on the critical Reynolds number of oscillatory flow. ($\hat{U}$ = mean velocity amplitude, U_0 = amplitude of axial velocity, $\delta = (2\nu/\omega)^{\frac{1}{2}}$.)

Several results, experimental and theoretical, on the critical Reynolds number are summarized in table 2. They are scattered over a relatively wide range. The reasons are as follows.

(*a*) First of all, the instability limits are sensitive to the base flow profile. Therefore there is no reason to believe that these experimental and theoretical results should be precisely compatible. Furthermore, a result of a two-dimensional theory cannot be compared with a counterpart of axisymmetric flow (as in the case of *steady* two-dimensional and axisymmetric Poiseuille flow). Disturbances in circular pipes may be asymmetric and three-dimensional.

(*b*) Experiments, except for those performed under rigorous control conditions, are susceptible to finite amplitude disturbances, which generally reduces the critical value.

(*c*) Discrepancies may be attributable partly to different transition criteria employed. In most experiments hitherto reported (e.g. Li 1954; Collins 1963), the instability limit was determined by visual observation of tracer dye, while in the present work direct measurements of velocity variation were carried out.

(*d*) The lower critical Reynolds number for the stability of modified Stokes layers on the bottom of water channels with travelling surface waves ($R_\delta^* = 160$; Collins 1963) may be the result of possible strong influence of the normal component of velocity and of the steady drift, as pointed out by von Kerczek & Davis (1974).

It is interesting to see that the critical Reynolds numbers for oscillatory pipe flows found by Sergeev (1966) and by the present authors (for the second transition) coincide, although in our experiments, transition to turbulence of the first type occurs at a significantly lower critical Reynolds number, which decreases with increasing λ.

Notwithstanding the item (*d*) mentioned above, the experimental critical Reynolds number found by Collins (1963) for two-dimensional oscillatory flow on a stationary plate compares relatively well with the theoretical one found by Hino & Sawamoto (1975*a*) for two-dimensional oscillatory flow between parallel plates at a high Stokes number λ, in which case the flow asymptotes to the case of Collins (1963).

REFERENCES

COLLINS, J. I. 1963 Inception of turbulence at the bed under periodic gravity waves. *J. Geophys. Res.* **18**, 6007–6014.

CONRAD, P. W. & CRIMINALE, W. O. 1965 *Z. angew. Math. Phys.* **16**, 233.

DAVIS, S. H. & VON KERCZEK, C. 1973 A reformulation of energy stability theory. *Arch. Rat. Mech. Anal.* **52**, 112–117.

EICHELBRENNER, E. A. (ed.) 1972 *Proc. IUTAM Symp. Recent Res. on Unsteady Boundary Layers*. Laval University Press.

HINO, M. & SAWAMOTO, M. 1975*a* Linear stability analysis of an oscillatory flow between parallel plates. *Proc. 7th Symp. on Turbulence* (ed. H. Sato & M. Ohji), pp. 1–7. Institute of Space and Aeronautics, University of Tokyo.

HINO, M. & SAWAMOTO, M. 1975*b* Experimental study on transition to turbulence in an oscillatory flow. *Dept. Civil Engng, Tokyo Inst. Tech. Tech. Rep.* no. 19.

HINO, M. & TAKASU, S. 1974 Experiments on turbulence in an oscillatory pipe flow. *Proc. 18th Conf. Hydraulic Research*, pp. 145–150. Japan Soc. Civil Engng.

KERCZEK, C. VON & DAVIS, S. H. 1972 The stability of oscillatory Stokes layers. *Studies in Appl. Math.* **51**, 239–252.

KERCZEK, C. VON & DAVIS, S. H. 1974 Linear stability theory of oscillatory Stokes layers. *J. Fluid Mech.* **62**, 753–773.

LI, H. 1954 Stability of oscillatory laminar flow along a wall. *Beach Erosion Bd, Corps Engrs, U.S.A., Tech. Memo.* no. 47.

MERKLI, P. & THOMANN, H. 1975 Transition to turbulence in oscillating pipe flow. *J. Fluid Mech.* **68**, 567–575.

RIEDEL, H. P., KAMPHUIS, J. W. & BREBNER, A. 1972 Measurements of bed shear stress under waves. *Proc. 13th Conf. Coastal Engng (Vancouver)*, pp. 587–603.

ROSENHEAD, L. (ed.) 1963 *Laminar Boundary Layers*. Oxford: Clarendon Press.

SERGEEV, S. I. 1966 Fluid oscillations in pipes at moderate Reynolds numbers. *Fluid Dyn. (Mekh. Zh.)*, **1**, 21–22.

VINCENT, G. E. 1957 Contribution to the study of sediment transport on a horizontal bed due to wave action. *Proc. 6th Conf. on Coastal Engng* (Florida), pp. 326–335.